

# Seismic Performance of RC Shear Wall Frames Considering Soil-Foundation-Structure Interaction

**S. Marzban**

*Bauhaus-Universität Weimar, Weimar, Germany*

**M. Banazadeh**

*Amirkabir University of Technology, Tehran, Iran*

**A. Azarbakht**

*Arak University, Arak, Iran*



## SUMMARY:

The Soil-Foundation-Structure Interaction (SFSI) is a complex phenomenon likely to have important effects on the seismic response of structures. In the present study, the “Beam on Nonlinear Winkler Foundation (BNWF)” approach was employed to investigate the inertial SFSI effects on the seismic performance of Concrete Shear Wall frames. Hence, frames of 3, 6, 10 and 15 number of stories founded on soft, medium and hard soils were designed and modeled in OpenSees. The resulting pushover curves were studied through two code-based viewpoints: 1) Force-Based Design and 2) Performance-Based Design. Finally, a comparison was made between the behavior of each frame element in the flexible-base and the fixed-base conditions. This paper demonstrates some degree of inaccuracy in the fixed-base assumption regularly applied in practice. Moreover, the results imply how the fixed based assumption overestimates the design of the shear wall element and underestimates the design of the connected moment frame.

*Keywords: Seismic Performance, RC Shear Wall Frames, Soil-Structure-Interaction*

## 1. INTRODUCTION

Pioneer studies in the field of Soil-Structure Interaction (SSI or in its more comprehensive form, Soil-Foundation-Structure Interaction, SFSI) were limited to the vibrations of machinery foundations and strategic structures such as reactors and oil tanks. However, providing advanced computing tools as well as new insights into the noticeable effects of SFSI on the behavior of building structures, today, interaction studies have also found their way in the investigation of these structures. With the development of the Performance-Based Earthquake Engineering and Design (PBEE and PBD) approaches, the need to incorporate the SFSI effects has gained even more attraction. Performance objects of interest in PBEE/PBD can be highly affected at the presence of complicated SFSI features. Several approaches are available for modeling the soil-foundation substructure. Two general categories can be roughly identified: micro and macro element methods. Obviously, micro-element approaches provide the most capabilities when simulating the SFSI. Yet, they are computationally costly and time-consuming [1]. This turns into a challenging concern when it comes to the uncertainty analysis where a large number of simulations is required. Indeed in this context, rather straightforward modeling methods facilitate the analysis process. Therefore, often in practical SFSI problems, application of simple methods such as Winkler approach is preferred. Winkler model, in simplest form, reduces the soil medium to a finite number of similar discrete and independent linear springs. Pacific Earthquake Engineering Research Center (PEER) released two reports [2, 3] in 2005 and 2007, with a concentration on the numerical modeling of surface foundations. Both reports attempted to introduce a practical application of the Winkler concept to nonlinear SFSI modeling. The proposed model consisted of vertical nonlinear independent springs, distributed along the foundation length and allowed for uplift, rocking, settlement and radiation damping. Considering its capabilities, this model was chosen to mainly account for the construction of the ‘beam on nonlinear Winkler foundation’ model in this study.

## 2. METHODOLOGY

Generally, the accuracy of the pushover analysis when predicting the structural performance is a matter of controversy. However, this simple method provides a useful understanding of the expected behavior of the structures [4]. Therefore, this study is based on the pushover analysis results. Primarily, lateral forces were applied to a group of selected Concrete Shear Wall (CSW) frames in the form of the recommended patterns of FEMA450 guidelines [5] with distributions relative to mass and height considering the effects of the higher modes. Later, the pushover curves were calculated and studied based on two methodologies according to design codes: Force-Based Design (FBD) and Performance-Based Design (PBD). The nonlinear dynamic analysis of coupled RC frame-wall systems in the absence/presence of SFSI is the subject of an ongoing research being carried out by the first author.

### 2.1. FBD Approach

In the FBD approach the bilinear ideal pushover curves were constructed and the two seismic design parameters, period-based ductility ( $\mu_T$ ) and overstrength coefficient ( $\Omega$ ), were determined based on FEMA695 guidelines [6]. Subsequently, the response modification coefficient ( $R$ ), was calculated. According to FEMA695 guidelines, the ideal bilinear curve was used to characterize the pushover curves, as schematically shown in Figure 2.1.  $\delta_{y,eff}$  and  $V_{max}$  designate the effective yield roof drift displacement and the maximum base shear resistance, respectively.  $\Omega$  and  $\mu_T$ , were then computed through equations  $\Omega = V_{max}/V$  and  $\mu_T = \delta_u/\delta_{y,eff}$  as specified in the mentioned guidelines where  $\delta_u$  corresponds to the ultimate roof displacement. In this procedure, the design base shear corresponding to a point of 'significant yield' in the pushover curve ( $V$ ), had to be identified. The occurrence of full yielding in the tensional boundary element of the shear wall was chosen to represent the significant yield point, based on a rational engineering judgment. Evidently, a similar explanation was not applicable to 3-story CSW frames due to their shear-dominant behavior. Hence,  $\Omega$  was not calculated for these frames. Eventually, the response modification factor ( $R$ ), was found according to Eqn. 2.1. and 2.2. in which  $V_E$  is the elastic seismic force demand and  $R_S$ ,  $R_\mu$  and  $R_R$  are the reduction coefficients due to structural over-strength, ductility and redundancy, respectively. It must be noted that  $R_R$  was the same for fixed-/flexible-base frames and was chosen to be one.

$$R_S = \Omega, R_\mu = \begin{cases} 1.0 & T \leq 0.03s \\ \sqrt{2\mu_T - 1} & 0.12s \leq T < 0.5s \\ \mu_T & 1.0s \leq T \end{cases} \quad (2.1)$$

$$R = V_E/V = R_S R_\mu R_R \quad (2.2)$$

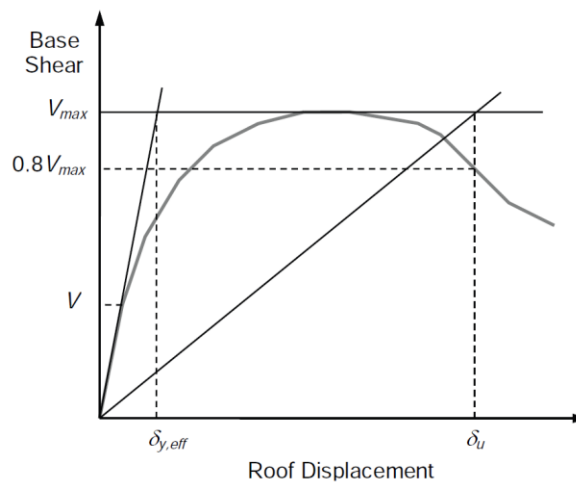


**Figure 2.1.** Idealized nonlinear static pushover curve based on FEMA695 guidelines [6].

## 2.2. PBD Approach

In the PBD approach the performance point was to be found by means of the Displacement Coefficients Method (DCM) based on FEMA273 guidelines [7]. *Equivalent displacements* approximation which forms the basis for the DCM implies that the method is only applicable to flexible structures. Moreover, the goal of this study was to obtain and compare the performance of fixed-/flexible-base CSW frames rather than to calculate the target displacement as a part of the design process. Therefore, each frame element was checked for three performance levels throughout the pushover analysis. The mentioned levels include Immediate Occupancy (IO), Life Safety (LS) and Collapse Prevention (CP), in accordance with FEMA356 guidelines [8]. It was assumed that a structural system has achieved a specific performance level if at least one of its members has already met that performance level. As a result, the performance levels of IO, LS and CP were determined and located on the pushover curves for each frame. Columns were not checked in this procedure. They were designed based on the strong column-weak beam concept them and hence were less vulnerable to the formation of the plastic hinges.

## 3. NUMERICAL MODELING

CSW frames with 3, 6, 10 and 15 stories and three spans were considered, as schematically shown in Figure 3.1. Hard, medium and soft soils were, in the same order, introduced through site classes B, C and D based on FEMA450 guidelines. With specified category and shear wave velocity for site classes, satisfactory values were estimated to represent their design parameters according to several well-known geotechnical references [9-16]. Selected values from the recommended ranges are presented in Table 3.1 wherein  $E$  modulus of elasticity,  $G$  shear modulus,  $\gamma$  specific weight,  $D_r$  relative density and  $\mu$  Poisson's ratio of the soil. It is necessary to note that uncertainties play an important role in the characterization of the soil behavior.

Gravity loads were selected based on values typically employed in engineering practice. Therefore, 3, 6, 10 and 15-story frames had masses equal to 307, 640, 927 and 1511 tons, respectively. Further, equivalent lateral design forces were determined based on FEMA450 guidelines i.e. the design spectrum for each site class was derived and the corresponding design base shears were calculated as presented in Table 3.2. Both gravity and seismic loads were later imposed on the frames according to the Additive and Counteractive load combinations of ASCE7-05 standard [17]. All frames were designed as special frames based on FEMA450 guidelines. Only 15-story frames had to be designed considering dual lateral resisting systems. Thickness of the shear wall was chosen to be 0.25 m in 3-/6-story frames and 0.30 m in 10-/15-story ones. Brief design details about the structural elements can be found in Table 3.3. Strip footings of width 2.0-4.6 m, length 19.6-20.0 m and fixed height 1.0 m, were designed for all frames. Fundamental periods of the designed elastic and the corresponding nonlinear models of the 3, 6, 10 and 15-story frames are presented in Table 3.4.

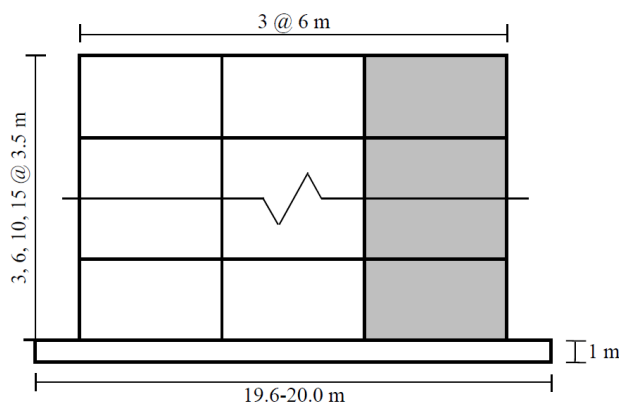


**Figure 3.1.** Schematic elevation of the studied frames.

**Table 3.1.** Selected characteristics for site classes B, C and D.

Soil Type	$E$ (MPa)	$G$ (MPa)	$\gamma$ ( $kN/m^3$ )	$D_r$ (%)	$\mu$
Rock	15000	6000	24	-	0.25
Gravel	200	74.1	21	85	0.35
Sand	65	24	19	75	0.35

**Table 3.2.** Calculated design base shears (kN).

Lateral Resisting System	No. of Stories	Site Class		
		B	C	D
Shear Wall Frame	10	700.4	873.1	990.8
	6	973.2	1048.7	1048.7
	3	503.3	503.3	503.3
Dual System (Shear Wall + Moment Resisting Frame)	15	557.2	725.0	835.8

**Table 3.3.** Brief design details of the studied frames.

No. of Stories	No. of Typical Stories (1 <sup>st</sup> Set along the Height)	Columns' Width (m)	$\rho_{sb}$	No. of Typical Stories (2 <sup>nd</sup> Set along the Height)	Columns' Width (m)	$\rho_{sb}$
3	3	0.45	0.012	-	-	-
6	3	0.45	0.024	3	0.45	0.012
10	4	0.55	0.019	3	0.45	0.024
15	4	0.70	0.016	4	0.60	0.016

All the columns have square cross sections. (Boundary elements have the same cross sectional dimensions as other columns.)

$\rho_{sb}$  corresponds to the ratio of reinforcement in the boundary element.

Vertical web reinforcement for all the frames:  $\phi 10 @ 20\text{cm}$

For 10 and 15 story frames only the details for the first 7 and 8 stories are presented, respectively.

**Table 3.4.** Fundamental fixed-base period of the frames (sec).

No. of Stories	Elastic model	Nonlinear Model
3	0.13	0.16
6	0.43	0.48
10	0.92	1.02
15	1.52	1.70

### 3.1. Moment-Resisting Frame Modeling

Beams with concentrated plastic hinges and columns of fiber section were employed to simulate the nonlinear flexural behavior of the moment frames. The nonlinear behavior for the plastic hinges was defined in accordance with Haselton et al. [18]. The backbone characterizing relationships are proposed in their study based on the calibration of numerous test results in the form of the suggested trilinear backbone curve by Ibarra [19,20]. This model is able to capture the softening due to concrete crushing, reinforcement buckling/yielding and bond slip, namely post cap behavior, in the negative stiffness region [18]. The trilinear Ibarra model, as discussed above, was introduced into the OpenSees platform using the Clough material proposed by Altoontash [21]. Columns were modeled by means of the fiber method with the capability of developing distributed plasticity along the element's length. This choice was made mostly due to the fact that the flexural behavior in columns is highly dependent on the interaction of their axial and bending forces. However, the aforementioned approach for beams was incapable of considering variable axial forces during the analysis.

### 3.2. Shear Wall Element Modeling

Recently, 'Flexure-Shear Interaction Displacement-Based Beam-Column' element has been developed in the OpenSees platform based on the concept of the widely used Multiple Vertical-Line-Element Model (MVLEM). Particularly, the new element is capable of taking the interaction between the flexural and shear behaviors into account. It was therefore selected to simulate the shear wall element in OpenSees considering its inclusive features. More information about the element can be found in Orakcal et al. [22]. The mid-panel of the shear wall was constructed with the above-mentioned

element while the boundary elements were modeled as columns of the main frame. Also, each element was divided into four sub-elements in a story level. Nodes located on the same elevation of the boundary elements and the mid-panel element were then joined by means of rigid beams. This scheme provided an integrated simulation of the whole shear wall system. As it is obvious, the constructed shear wall model could benefit from the top features of both the flexure-shear interaction model and the fiber section.

### 3.3. Soil-Footing Interface Modeling

The Beam on Nonlinear Winkler Foundation (BNWF) was employed to model the soil-footing interface. This model is not also able to simulate the uplift and rocking motions (geometrical nonlinearity) but also the nonlinear behavior of the soil (material nonlinearity). Furthermore, it allows for uneven stiffness and spacing assignments to the soil springs along the foundation length. It is worth mentioning that the beam at the base of the shear wall was set to be rigid due to high flexural stiffness that the shear wall adds to the footing's rigidity. The footing was constrained against sliding [3, 23, 24]. In order to define the nonlinear Winkler springs, the strength and stiffness of the springs had to be identified. The Gazetas concentrated stiffness [25] was employed to define the stiffness of the soil springs. Initially, the total vertical and rotational stiffness of the footing-soil systems were found according to Gazetas proposed relations as shown in Table 3.5. A specific distribution of Winkler springs was later selected for each system to produce the same total vertical and rotational concentrated stiffness [2]. Different stiffness contributions were considered for the springs in the middle and end regions of the footing. More stiff springs were placed at the ends of the footing strip to supply the rotational stiffness of the soil-footing system [2]. The end lengths were determined based on [2]. Likewise, the strength of the Winkler springs was calculated based on the bearing capacity of the foundations. Among several equations available to determine the bearing capacity, Meyerhof's equation (1963), a rigorously developed edition of Terzaghi's relation, [9], was selected to estimate the foundation bearing capacities in this study as presented in Table 3.6.

**Table 3.5.** The soil-footing elastic vertical/rotational Gazetas stiffnesses.

Stiffness Intensity	Number of stories				
	Site class	3	6	10	15
$Vertical = \frac{K_z}{A}$ ( $\frac{MN}{m^3}$ )	B	5419	3708	2882	2574
	C	77	53	41	37
	D	25	17	13	12
$Rotational = \frac{K_{\theta_y}}{I_y}$ ( $\frac{MN.m}{m^4}$ )	B	7697	6545	5744	5432
	C	110	93	82	77
	D	36	30	27	25

**Table 3.6.** Foundation bearing capacity based on Meyerhof's relationship.

Foundation bearing capacity	Number of stories				
	Site class	3	6	10	15
$q_{ult}$ (kPa)	B	49304	61931	75183	83381
	C	14526	17629	20967	22989
	D	5291	6227	7267	7886

## 4. NONLINEAR STATIC ANALYSIS RESULTS

Before the lateral load was applied, Additive and Counteractive Vertical Loadings (AVL and CVL) were separately imposed on the frames according to the load combinations discussed in section 3. Settlement due to gravity was also considered in case of the flexible-base models. An increase could be observed in the flexible-base fundamental period due to the contribution of the rocking motion in the first mode. This was particularly evident in lower height frames founded on softer soils. For instance the 3-story frame on site class D had a flexible-base period of more than two times that of the fixed-base. Although, the observed increase tended to disappear for the cases of stiffer soils and/or more flexible frames.

#### 4.1. Study of pushover curves based on FBD codes

The approximate bilinear pushover curves were calculated according to FEMA695 guidelines, as seen in Figure 4.2 for 3/15-story frames. The SFSI significantly decreases the initial stiffness of all frames. This substantiates the fundamental period elongation. However, higher (i.e. more flexible) frames are less affected in this regard. Also it is noteworthy to mention that the total seismic capacity remains approximately the same, when transforming from fixed to flexible-base condition. Namely, the SFSI does not alter the total base shear capacity but rather makes it occur at larger overall displacements. Further, the influence of the gravity loads on the SFSI was examined. Footing uplift is assumed to be more likely when the structure is under lower gravity loads. Here, it is found that low-rise frames (3/6-story) under CVL are more affected by the SFSI than those frames under AVL. This trend, however, gets reversed for high-rise frames (10/15-story), i.e. SFSI affects frames with AVL more than those with CVL. In the former case, lower gravity loads tend to undermine the overall stability of the structural system and thus result in less effectiveness of the SFSI in contradiction to low-rise frames.

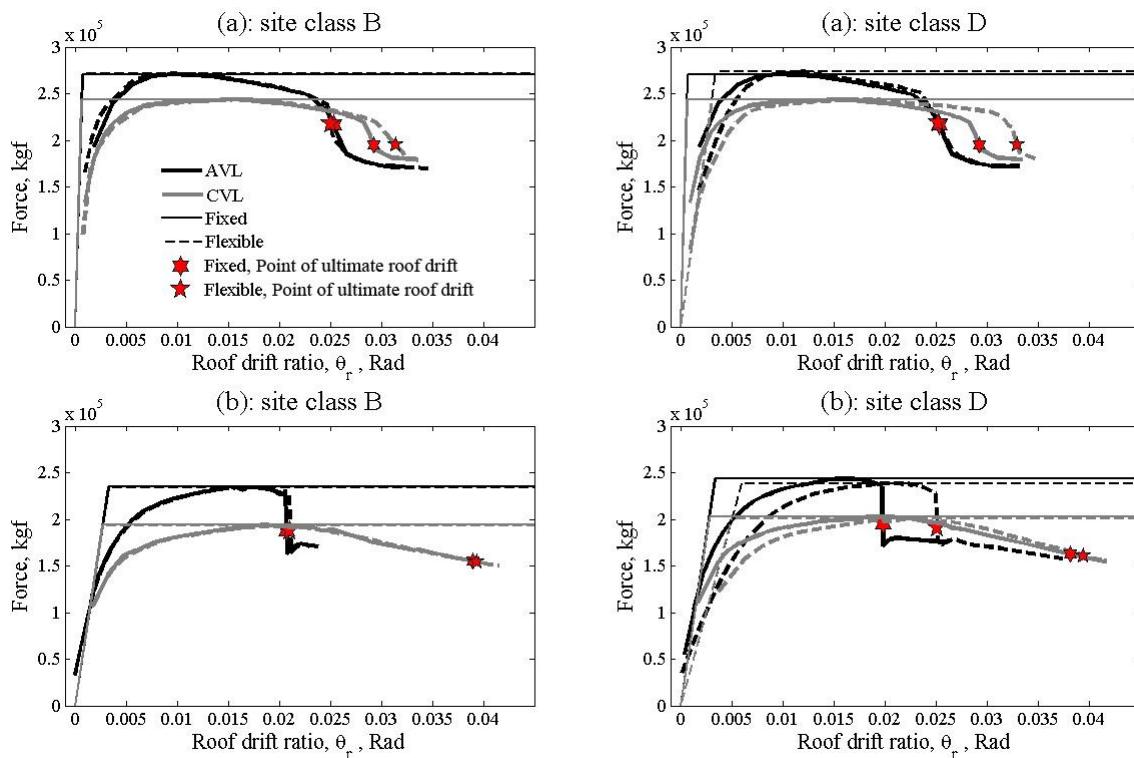


**Figure 4.2.** Pushover curves and their bilinear idealization for (a) 3 and (b) 15-story frames founded on site classes B and D.

Following FEMA695 guidelines, the period-based ductility,  $\mu_T$  was calculated as seen in Figure 4.3(a). It is clearly recognized that the SFSI substantially reduces  $\mu_T$ . Also, relatively large differences are observed between the ductilities on rigid (B) and non-rigid (C and D) soils. Accordingly, rigid base assumption for frames founded on non-rigid soils can lead to a misestimating of the  $\mu_T$ . Again, as it is expected, the descending inclination flattens when frames are more flexible. Next, the overstrength coefficient was calculated. As discussed previously, the overstrength coefficient was not computed for 3-story frames because of their shear-dominant behavior. Hence, Figure 4.3(b) shows the values of  $\Omega$  for 6, 10 and 15-story frames. It is clear that changes in  $\Omega$  due to SFSI are not much of concern.

Ductility and overstrength coefficients were later employed to determine  $R_\mu$  and  $R$  as shown in Figure 4.4. It can be observed that  $R$  decreases noticeably in CSW frames with SFSI when compared to fixed-base frames. Also, there is a clear downward trend for  $R$  from hard to soft soils. Again, large differences are seen between the reduction factors on rigid and non-rigid soils. Namely, the rigid base assumption may not result in true values for  $R$  in the case of frames founded on non-rigid soils. The

same descending trend for  $R$  cannot be recognized for 6-story frames because their fundamental periods fell in the transition area between the constant acceleration and velocity regions of the response spectra. Thus different equations for  $R_\mu$  were utilized. Concerning the above discussions, it can be concluded that the fixed-base assumption has to be used quite cautiously. The design practitioner should be aware that the flexible-base assumption elongates the fundamental period on one hand but it also reduces the reduction factor  $R$  on the other hand.

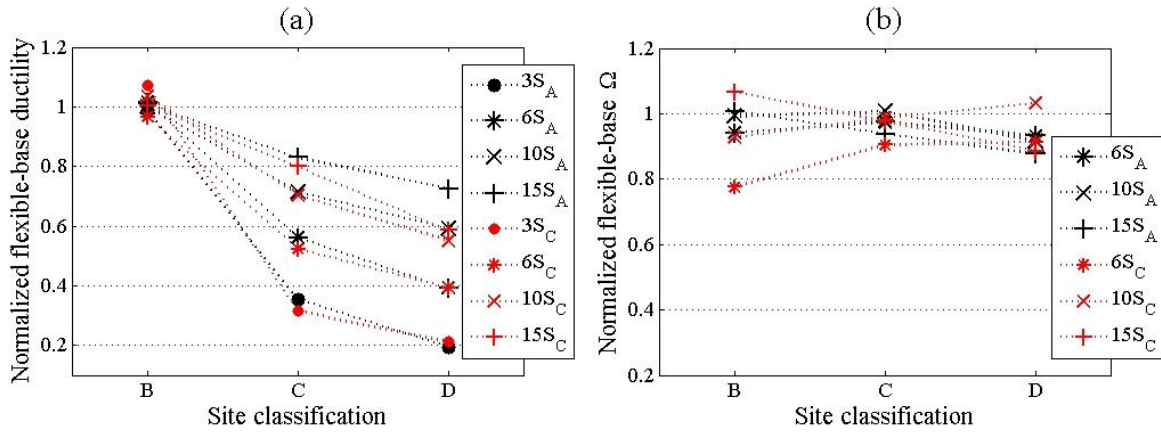


**Figure 4.3.** The normalized (a) period-based ductility ( $\frac{\mu_{T(Flexible)}}{\mu_{T(Fixed)}}$ ) (b) overstrength coefficient ( $\frac{\Omega_{(Flexible)}}{\Omega_{(Fixed)}}$ ).

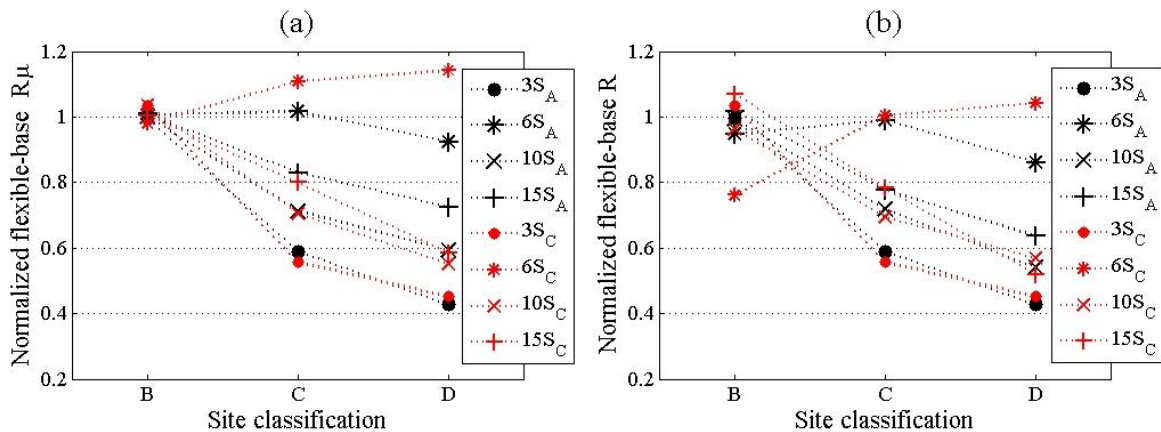


**Figure 4.4.** The normalized (a) ductility reduction coefficient ( $\frac{R_{\mu(Flexible)}}{R_{\mu(Fixed)}}$ ) (b) reduction factor ( $\frac{R_{(Flexible)}}{R_{(Fixed)}}$ ).

## 4.2. Study of pushover curves based on PBD codes

IO, LS and CP performance levels were determined for each of the beams plastic hinges and the shear wall elements, based on FEMA356 guidelines. The detected performance levels for the members were later used to locate the performance points of the whole systems on the corresponding pushover curves. Selected results are shown in Figure 4.5 for the frames located on site class D.

According to the figure, seismic performance is generally improved in the flexible-base state. As expected, improvements are extended when soil loses stiffness from site class B to site class D. Although, this is not the case for 10-story frame under CVL. It should be noted that, 10-story frames were not designed as dual lateral resisting systems based on FEMA450 guidelines. Hence, moment frames were solely designed to withstand gravity loads in 10-story frames. On the other hand, it is obvious from the results that in the flexible-base state, moment frames contribute more to the lateral resisting of the systems when compared to the fixed-base condition. This is specifically true for higher frames. Consequently, in the case of flexible-base 10-story frame, the moment frame was loaded

beyond its design forces and deformations. Therefore, it failed to provide a reasonable behavior and plastic hinges were formed at lower loading steps. Nevertheless, 10-story frame under AVL does not follow the same trend. That is because of more stability due to larger gravity loads and thus, less tendency to deform.

Furthermore, performance of the shear walls is improved in the flexible-base cases. Namely, a certain performance level was attained under the application of a larger force in the flexible-base state when compared to the fixed-base condition. As it is expected the trend is not the case for flexible-based 10-story frames owing to the weak performance of the connected moment frames. Finally, it is hard to find a general trend for the performance of the beams plastic hinges. Nonetheless, for low-rise frames the SFSI tends to weaken the performance. For 15-story frames, however, a certain performance level is achieved at a larger displacement when SFSI is considered. The special case for 10-story frames is formerly discussed.

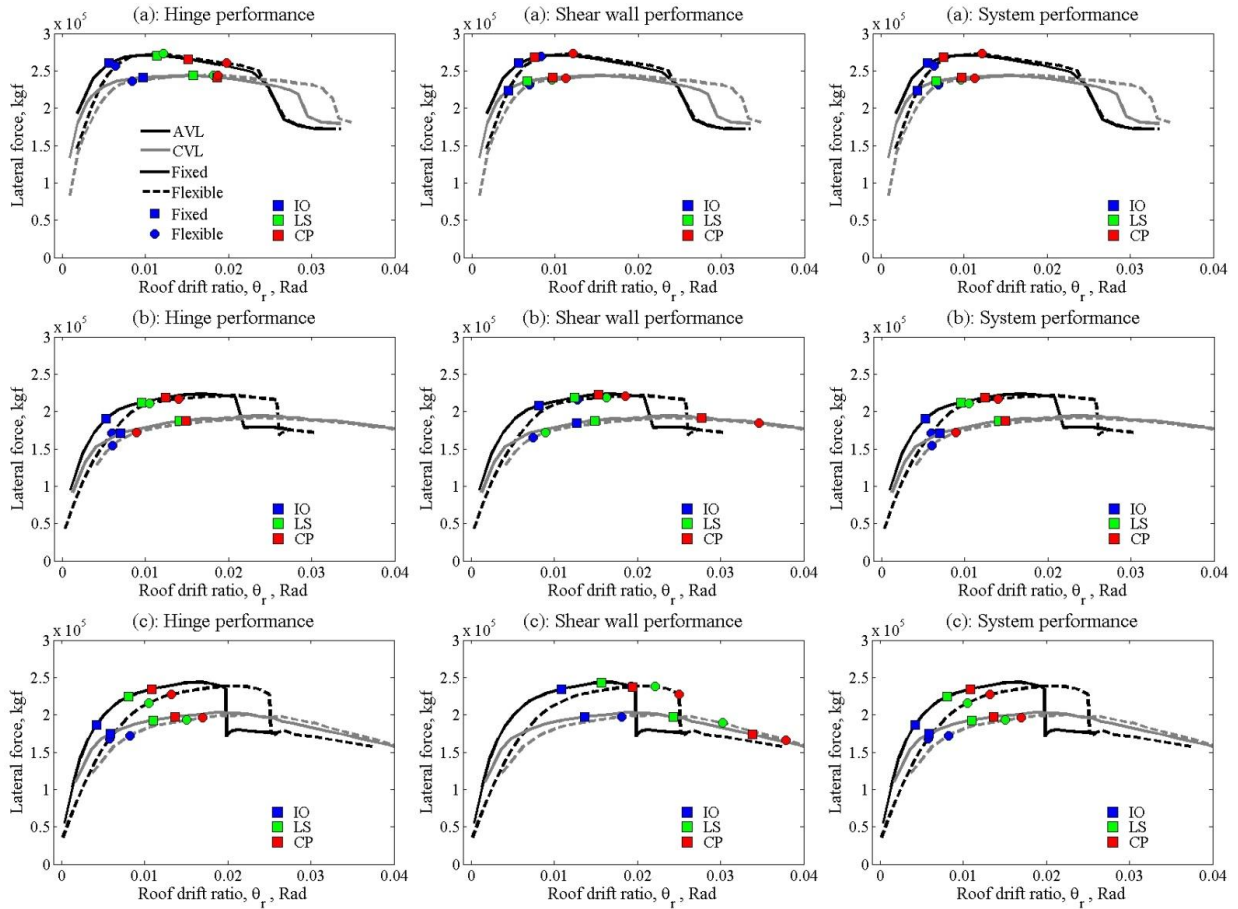


**Figure 4.5.** Plastic hinges, shear wall element and the overall performance of (a) 3, (b) 10 and (c) 15-story frames founded on site class D.

## 5. CONCLUSIONS

The seismic response of a selected number of CSW frames was assessed in the presence of SFSI through static nonlinear analysis. The nonlinear beam on Winkler foundation was used to represent the soil-footing substructure. 3, 6, 10 and 15 story CSW frames founded on soft, medium and hard soils were considered. Through a force-based code approach the seismic design parameters were determined for flexible and fixed-base frames. It was found that as the soil flexibility increased the reduction factor  $R$  decreased whereas the fundamental period increased. Hence, it is suggested that careful attention be paid to the newly introduced design conditions in which the reduced reduction factor and increased fundamental period inversely impact on the estimated design lateral force.

In addition, the seismic performance of CSW frames was studied through a performance-based code

approach. In general, the overall seismic performance of the frames was enhanced in all the studied cases except for the 10-story frames under low level of gravity loads. In the latter case, the moment resisting frame failed to efficiently involve in providing the lateral resistance, mainly because according to FEMA450 guidelines it was designed to withstand gravity loads only. Consequently, the shear wall element and the beam plastic hinges presented weak performance in 10-story frames. In contrast, the shear wall performance was enhanced in all other cases. Yet, the plastic hinges did not follow a noticeable trend. Nevertheless, one could roughly generalize that the SFSI degraded the plastic hinges performance in the low-rise frames while in the high-rise ones it got reversed.

In the final analysis, it should be noted that the SFSI consequences on the seismic performance of CSW frames account for far more crucial considerations than the period elongation alone. In fact the use of the fixed-base assumption may lead to errors in the evaluation of the real structural forces and displacements. As it was used in this paper, the Winkler model can provide a simple yet sufficiently accurate solution to the SFSI problems, demanding less costs and time.

As it was mentioned in section 2, a comprehensive study on the seismic damage assessment of coupled frame-wall systems is currently being carried out by the first author. Since the formerly applied model for the shear walls is only validated under monotonic loading conditions [22] an improved modeling approach is to be used. Global model quality evaluation of the aforementioned frame-wall systems is the subject of the current research.

#### ACKNOWLEDGEMENT

The first author is currently a member of the Research Training Group 1462 (GRK 1462) at the Faculty of Civil Engineering, Bauhaus University of Weimar. The ongoing research is funded by the German Research Foundation (DFG). This support is gratefully acknowledged.

#### REFERENCES

- [1] Allotey, N., & El Naggar, M. H. (2008). An investigation into the Winkler modeling of the cyclic response of rigid footings. *Soil dynamics & earthquake engineering* , **28:1**, 44-57.
- [2] Harden, C., Hutchinson, T. C., Martin, G. R., & Kutter, B. L. (2005). *Numerical modeling of the nonlinear cyclic response of shallow foundations*. Report No. PEER-2005/04. Berkeley: Pacific Earthquake Engineering Research Center, University of California.
- [3] Gajan, S., Hutchinson, T. C., Kutter, B. L., Raychowdhury, P., Ugalde, J. A., & Stewart, J. P. (2007). *Numerical models for analysis and performance-based design of shallow foundations subjected to seismic loading*. Report No. PEER-2007/04. Berkeley: Pacific Earthquake Engineering Research Center, University of California.
- [4] Vamvatsikos, D., & Fragiadakis, M. (2009). Incremental dynamic analysis for estimating seismic performance sensitivity and uncertainty. *Earthquake engineering & structural dynamics* , **39:2**, 141-163.
- [5] FEMA, (2004). *NEHRP Recommended Provisions for Seismic Regulations for New Buildings and Other Structures*, FEMA 450-1/2003 Edition, Part 1: Provisions, Federal Emergency Management Agency, Washington, D.C.
- [6] FEMA, (2009). *Quantification of Building Seismic Performance Factors*, FEMA P695/2009 Edition, Federal Emergency Management Agency, Washington, D.C.
- [7] Building Seismic Safety Council (BSSC, 1997a). *FEMA 273/274 - NEHRP Guidelines for the Seismic Rehabilitation of Buildings*, Vol. I – Guidelines, Vol. II – Commentary, Washington, DC.
- [8] FEMA, (2000). *Prestandard and Commentary for Seismic Rehabilitation of Buildings*, FEMA 356, Prepared by the American Society of Civil Engineers for the Federal Emergency Management Agency, Washington, D.C.
- [9] Bowles, J. E. (1997). *Foundation analysis and design* (5th ed.). London: McGraw-Hill.
- [10] Day, R. W. (2002). *Geotechnical earthquake engineering handbook*. McGraw-Hill.
- [11] Day, R. W. (2006). *Foundation engineering handbook: design and construction with the 2006 international building code*. McGraw-Hill.
- [12] Bell, F. G. (2000). *Engineering properties of soils and rocks* (4th ed.). Wiley-Blackwell.
- [13] Hunt, R. E. (2005). *Geotechnical engineering investigation handbook* (2nd ed.). CRC Press.
- [14] Das, B. M. (2006). *Principles of geotechnical engineering* (6th ed.). Thomson.
- [15] Brown, R. W. (2001). *Practical foundation engineering handbook* (2nd ed.). McGraw-Hill.
- [16] Murthy, V. N. (2003). *Geotechnical engineering: principles and practices of soil mechanics and foundation engineering*. CRC Press.

- [17] American Society of Civil Engineers, (2005). *Minimum Design Loads for Buildings and Other Structures*, ASCE/SEI 7-05.
- [18] Haselton, C. B., S. Taylor Lange, A. B. Liel, and G. G. Deierlein (2007). *Beam-Column Element Model Calibrated for Predicting Flexural Response Leading to Global Collapse of RC Frame Buildings*, Report No. PEER-2007/03. Berkeley: Pacific Engineering Research Center, University of California.
- [19] Ibarra, L. (2003). *Global collapse of frame structures under seismic excitations*. (PhD thesis). Department of CEE, Stanford University, USA.
- [20] Ibarra, L. F., Medina, R. A., & Krawinkler, H. (2005). Hysteretic models that incorporate strength and stiffness deterioration. *Earthquake engineering & structural dynamics* , **34:12**, 1489-1511.
- [21] Altoontash, A. (2004). *Simulation and damage models for performance assessment of reinforced concrete beam- column joints*. (PhD thesis). Department of Civil and Environmental Engineering, Stanford University.
- [22] Orakcal, K., Massone, L., Wallace, J. (2006). *Analytical modeling of reinforced concrete walls for predicting flexural and coupled- shear- flexural response*. Report No. PEER-2006/07. Berkeley: Pacific Earthquake Engineering Research Center, University of California.
- [23] Beucke, K., Werkle, H., & Waas, G. (1983). Nonlinear soil-structure-interaction with base mat uplift. *7th international conference on structural mechanics in reactor technology*. Chicago.
- [24] Xu, C. J., & Spyrakos, C. C. (1996). Seismic Analysis of towers including foundation uplift. *Engineering structures* , **18:4**, 271-278.
- [25] Gazetas, G. (1991). Foundation Vibrations. In H. Y. Fang (Ed.), *Foundation engineering handbook* (pp. 553-593). New York: Van Nostrand Reinhold.